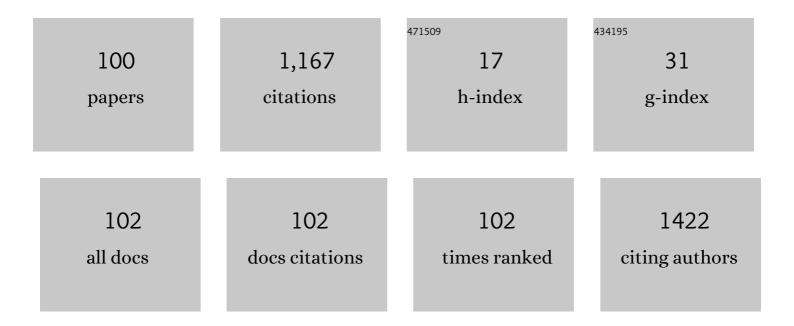
List of Publications by Year in descending order

Source: https://exaly.com/author-pdf/3629042/publications.pdf Version: 2024-02-01



#	Article	IF	CITATIONS
1	Magnesium doped semipolar (11–22) p-type gallium nitride: Impact of dopant concentration variants towards grain size distributions and crystalline quality. Thin Solid Films, 2022, 741, 139003.	1.8	3
2	Effect of Flux Rate Variation at Fixed V/III Ratio on Semi-Polar (112Â <sup>-</sup> 2) GaN: Crystal Quality and Surface Morphology Study. Crystals, 2022, 12, 247.	2.2	2
3	Non-Polar Gallium Nitride for Photodetection Applications: A Systematic Review. Coatings, 2022, 12, 275.	2.6	13
4	Improved performance of InGaN/GaN LED by optimizing the properties of the bulk and interface of ITO on p-GaN. Applied Surface Science, 2021, 540, 148406.	6.1	5
5	The effect of Multi Quantum Well growth regime transition on MQW/p-GaN structure and light emitting diode (LED) performance. Materials Science in Semiconductor Processing, 2021, 121, 105431.	4.0	5
6	Disilane doping of semi-polar (11-22) n-GaN: The impact of terrace-like evolution toward the enhancement of the electrical properties. Thin Solid Films, 2021, 720, 138489.	1.8	1
7	The crystallographic quality and band-edge transition of as-deposited PALE AlN films via metal organic chemical vapor deposition. Journal of Materials Science: Materials in Electronics, 2021, 32, 3211-3221.	2.2	2
8	Diminishing the Induced Strain and Oxygen Incorporation on Aluminium Nitride Films Deposited Using Pulsed Atomic-Layer Epitaxy Techniques at Standard Pressure MOCVD. Journal of Electronic Materials, 2021, 50, 2313-2322.	2.2	5
9	Impact of crystallinity towards the performance of semi-polar (11–22) GaN UV photodetector. Materials Letters, 2021, 286, 129244.	2.6	9
10	Effect of indium pre-flow on wavelength shift and crystal structure of deep green light emitting diodes. Optical Materials Express, 2021, 11, 926.	3.0	4
11	Impact of sandwiched strain periodic multilayer AlN/GaN on strain and crystalline quality of a-plane GaN. Scientific Reports, 2021, 11, 9724.	3.3	3
12	Enhanced indium adsorption and surface evolution of semi-polar (11–22) LED via a strain periodic alternating superlattice (SPAS-L). Materials Today Communications, 2021, 27, 102441.	1.9	2
13	Structural and mechanical properties of a-axis AlN thin films growth using reactive RF magnetron sputtering plasma. Microelectronics International, 2021, 38, 99-104.	0.6	0
14	Effect of nucleation layer thickness on reducing dislocation density in AlN layer for AlGaN-based UVC LED. Microelectronics International, 2021, 38, 113-118.	0.6	1
15	The optimization of n-type and p-type m-plane GaN grown on m-plane sapphire substrate by metal organic chemical vapor deposition. Materials Science in Semiconductor Processing, 2021, 131, 105836.	4.0	10
16	Improvement of c-axis (002) AlN crystal plane by temperature assisted HiPIMS technique. Microelectronics International, 2021, 38, 86-92.	0.6	1
17	Luminescence and Crystalline Properties of InGaN-based LED on Si Substrate with AlN/GaN Superlattice Structure. Journal of Physical Science, 2021, 32, 1-11.	0.9	1
18	Electronic surface, optical and electrical properties of p – GaN activated via in-situ MOCVD and ex-situ thermal annealing in InGaN/GaN LED. Materials Science in Semiconductor Processing, 2020, 106, 104757.	4.0	0

#	Article	IF	CITATIONS
19	Positioning of periodic AlN/GaN multilayers: Effect on crystalline quality of a-plane GaN. Materials Science in Semiconductor Processing, 2020, 105, 104700.	4.0	15
20	Poly(3-hexylthiophene-2,5-diyl) regioregular (P3HT) thin film as saturable absorber for passively Q-switched and mode-locked Erbium-doped fiber laser. Optical Fiber Technology, 2020, 54, 102073.	2.7	17
21	Indium tin oxide coated D-shape fiber as saturable absorber for passively Q-switched erbium-doped fiber laser. Optics and Laser Technology, 2020, 124, 105998.	4.6	23
22	Alq 3 saturable absorber for generating Qâ€switched pulses in erbiumâ€doped fiber laser. Microwave and Optical Technology Letters, 2020, 62, 1028-1032.	1.4	1
23	Influence of post-ammonia annealing temperature on e-beam evaporation deposited GaN layer on patterned sapphire substrate. Superlattices and Microstructures, 2020, 148, 106722.	3.1	1
24	Indium Tin Oxide Coated D-Shape Fiber as a Saturable Absorber for Generating a Dark Pulse Mode-Locked Laser*. Chinese Physics Letters, 2020, 37, 054202.	3.3	24
25	MEH-PPV organic material as saturable absorber for Q-switching and mode-locking applications. Journal of Modern Optics, 2020, 67, 746-753. Growth of semi-polar <mml:math <="" td="" xmlns:mml="http://www.w3.org/1998/Math/MathML"><td>1.3</td><td>5</td></mml:math>	1.3	5
26	Growth of semi-polar <mml:math <br="" xmlns:mml="http://www.w3.org/1998/Math/MathML">altimg="si1.svg"&gt;<mml:mrow><mml:mrow><mml:mo stretchy="true"&gt;(<mml:mrow><mml:mn>11</mml:mn><mml:mrow><mml:mover) 0="" etqq0="" rge<="" td="" tj=""><td>T /Qverloc</td><td>ck 10 Tf 50 46</td></mml:mover)></mml:mrow></mml:mrow></mml:mo </mml:mrow></mml:mrow></mml:math>	T /Qverloc	ck 10 Tf 50 46
27	In-Situ Multiple Ammonia Treatment (I-SMAT) method. Vacuum, 2020, 174, 109208. Mode-locked erbium-doped fiber laser via evanescent field interaction with indium tin oxide. Optical Fiber Technology, 2020, 55, 102124.	2.7	15
28	Crystal quality and surface structure tuning of semi-polar (11–22) GaN on m-plane sapphire via in-situ multiple ammonia treatment. Thin Solid Films, 2020, 697, 137817.	1.8	12
29	Agglomeration enhancement of AlN surface diffusion fluxes on a (0 0 0 1)-sapphire substrate grown by pulsed atomic-layer epitaxy techniques <i>via</i> MOCVD. CrystEngComm, 2020, 22, 3309-3321.	2.6	7
30	Anodization voltage effect on physical properties of anodic TiO2 nanotube arrays film. AIP Conference Proceedings, 2020, , .	0.4	0
31	Impact of a Strained Periodic Multilayer on the Surface and Crystal Quality of a Semipolar (11–22) GaN Template. Crystal Growth and Design, 2019, 19, 6092-6099.	3.0	9
32	Effects of pulse cycle number on the quality of pulsed atomic-layer epitaxy AlN films grown via metal organic chemical vapor deposition. Japanese Journal of Applied Physics, 2019, 58, SC1037.	1.5	8
33	Surface and optical characteristics of polycrystalline GaN layer with different pores profile of porous GaAs/GaAs substrate. Materials Research Express, 2019, 6, 085906.	1.6	0
34	Solution-Processable Vertical Organic Light-Emitting Transistors (VOLETs) with Directly Deposited Silver Nanowires Intermediate Source Electrode. Journal of Nanoscience and Nanotechnology, 2019, 19, 6995-7003.	0.9	6
35	Fabrication of In <sub>x</sub> Ga <sub>1-x</sub> N/GaN Multi-Quantum well Structure for Green Light Emitting Diode on Patterned Sapphire Substrate by Metal Organic Chemical Vapour Deposition. Solid State Phenomena, 2019, 290, 147-152.	0.3	1
36	In-situ tuning of Sn doped In2O3 (ITO) films properties by controlling deposition Argon/Oxygen flow. Applied Surface Science, 2019, 479, 1220-1225.	6.1	17

#	Article	IF	CITATIONS
37	Ammonia flux tailoring on the quality of AlN epilayers grown by pulsed atomic-layer epitaxy techniques on (0 0 0 1)-oriented sapphire substrates <i>via</i> MOCVD. CrystEngComm, 2019, 21, 2009-2017.	2.6	21
38	Improving Material Quality of Polycrystalline GaN by Manipulating the Etching Time of a Porous AlN Template. Journal of Electronic Materials, 2019, 48, 3547-3553.	2.2	1
39	Effect of the Bias Voltage on the Polycrystalline a-axis Oriented AlN Thin Films by RF Sputtering. , 2019, , .		0
40	Enhancement of optical transmittance and electrical resistivity of post-annealed ITO thin films RF sputtered on Si. Applied Surface Science, 2018, 443, 544-547.	6.1	80
41	Thermally Resistive Electrospun Composite Membranes for Lowâ€Grade Thermal Energy Harvesting. Macromolecular Materials and Engineering, 2018, 303, 1700482.	3.6	6
42	Effect of thermal interaction between bulk GaN substrates and corral sapphire on blue light emission InGaN/GaN multi-quantum wells by MOCVD. Superlattices and Microstructures, 2018, 119, 157-165.	3.1	3
43	Effect of low NH3 flux towards high quality semi-polar (11-22) GaN on m-plane sapphire via MOCVD. Superlattices and Microstructures, 2018, 117, 207-214.	3.1	20
44	Metal organic chemical vapor deposition of m-plane GaN epi-layer using a three-step approach towards enhanced surface morphology. Thin Solid Films, 2018, 667, 48-54.	1.8	5
45	Standard pressure deposition of crack-free AlN buffer layer grown on c-plane sapphire by PALE technique via MOCVD. Superlattices and Microstructures, 2018, 120, 319-326.	3.1	10
46	Embedded AlN/GaN multi-layer for enhanced crystal quality and surface morphology of semi-polar (11-22) GaN on m-plane sapphire. Materials Science in Semiconductor Processing, 2018, 86, 1-7.	4.0	14
47	Effect of working power and pressure on plasma properties during the deposition of TiN films in reactive magnetron sputtering plasma measured using Langmuir probe measurement. Journal of Physics: Conference Series, 2018, 995, 012068.	0.4	1
48	Observation of saturation transfer characteristics in solution processed vertical organic field-effect transistors (VOFETs) with high leakage current. Current Applied Physics, 2018, 18, 1415-1421.	2.4	12
49	Correlation between indium content in monolithic InGaN/GaN multi quantum well structures on photoelectrochemical activity for water splitting. Journal of Alloys and Compounds, 2017, 706, 629-636.	5.5	16
50	Optimization of poly(vinylidene fluoride) membranes for enhanced power density of thermally driven electrochemical cells. Journal of Materials Science, 2017, 52, 10353-10363.	3.7	11
51	Fabrications of Nanocomposite Gold-Polymer Metamaterials Consisting of Periodic Microcavities with Tunable Optical Properties. Optik, 2017, 150, 54-61.	2.9	1
52	Development of atmospheric pressure plasma needle jet for sterilization applications. AIP Conference Proceedings, 2017, , .	0.4	2
53	Nitrogen emission in reactive magnetron sputtering plasmas during the deposition of titanium nitride thin film. AIP Conference Proceedings, 2017, , .	0.4	0
54	Synthesis and characterization of InN nanocrystals on glass substrate by plasma assisted reactive evaporation. AIP Conference Proceedings, 2017, , .	0.4	0

#	Article	IF	CITATIONS
55	Fabrication of nanostructured Al-doped ZnO thin film for methane sensing applications. AIP Conference Proceedings, 2016, , .	0.4	0
56	Effect of nitridation surface treatment on silicon (1 1 1) substrate for the growth of high quality single-crystalline GaN hetero-epitaxy layer by MOCVD. Applied Surface Science, 2016, 362, 572-576.	6.1	25
57	High figure of merit of the post-annealed Ti/Al/ITO transparent conductive contacts sputter deposited on n-GaN. Journal of Alloys and Compounds, 2016, 681, 186-190.	5.5	9
58	First-principles calculation of structural, optoelectronic properties of the cubic Al Ga In1 N quaternary alloys matching on AlN substrate, within modified Becke–Johnson (mBJ) exchange potential. Optik, 2016, 127, 11577-11587.	2.9	5
59	High Thermal Gradient in Thermo-electrochemical Cells by Insertion of a Poly(Vinylidene Fluoride) Membrane. Scientific Reports, 2016, 6, 29328.	3.3	33
60	Effect of Sn dopant concentration on structural and electrical properties of ZnO nanostructures based methane gas sensor. , 2015, , .		0
61	Structural ordering, morphology and optical properties of amorphous Al In1â^'N thin films grown by plasma-assisted dual source reactive evaporation. Journal of Alloys and Compounds, 2015, 632, 741-747.	5.5	17
62	Investigation of the electrochemical behavior of indium nitride thin films by plasma-assisted reactive evaporation. RSC Advances, 2015, 5, 17325-17335.	3.6	27
63	One-pot sol–gel synthesis of reduced graphene oxide uniformly decorated zinc oxide nanoparticles in starch environment for highly efficient photodegradation of Methylene Blue. RSC Advances, 2015, 5, 21888-21896.	3.6	116
64	Effect of using two-step thermal annealing with different ambient gas on Mg activation and crystalline quality in GaN. Superlattices and Microstructures, 2015, 82, 592-598.	3.1	8
65	Crystalline quality assessment, photocurrent response and optical properties of reduced graphene oxide uniformly decorated zinc oxide nanoparticles based on the graphene oxide concentration. RSC Advances, 2015, 5, 53117-53128.	3.6	40
66	Modeling and simulation of metal organic halide vapor phase epitaxy (MOHVPE) growth chamber. Microsystem Technologies, 2015, 21, 309-318.	2.0	0
67	Nanocolumnar zinc oxide as a transparent conductive oxide film for a blue InGaN-based light emitting diode. Ceramics International, 2015, 41, 913-920.	4.8	9
68	Improved optoelectronics properties of ITO-based transparent conductive electrodes with the insertion of Ag/Ni under-layer. Applied Surface Science, 2014, 315, 387-391.	6.1	12
69	Plasma-assisted hot filament chemical vapor deposition of AlN thin films on ZnO buffer layer: toward highly c-axis-oriented, uniform, insulative films. Applied Physics A: Materials Science and Processing, 2014, 117, 2217-2224.	2.3	24
70	Effect of Substrate Temperature on Structural and Morphological Properties of Indium Tin Oxide Nanocolumns Using RF Magnetron Sputtering. Advanced Materials Research, 2014, 895, 12-16.	0.3	1
71	Structural and Optical Properties of Nickel (Ni)/indium Tin Oxide (ITO) Thin-Films Deposited by RF Magnetron Sputtering. Advanced Materials Research, 2014, 895, 181-185.	0.3	1
72	The effect of sputtering pressure on structural, optical and electrical properties of indium tin oxide nanocolumns prepared by radio frequency (RF) magnetron sputtering. Superlattices and Microstructures, 2014, 72, 140-147.	3.1	15

#	Article	IF	CITATIONS
73	Synthesis and characterization of ZnO NPs/reduced graphene oxide nanocomposite prepared in gelatin medium as highly efficient photo-degradation of MB. Ceramics International, 2014, 40, 10217-10221.	4.8	131
74	Effects of graphene oxide concentration on optical properties of ZnO/RGO nanocomposites and their application to photocurrent generation. Journal of Applied Physics, 2014, 116, .	2.5	132
75	Numerical estimation of self-sputtering effect in ionized physical vapor deposition system. , 2014, , .		Ο
76	Effects of Growth Temperature on the Structural Properties of Zinc Oxide Nanograins Deposited by RF Magnetron Sputtering. Advanced Materials Research, 2014, 895, 500-504.	0.3	0
77	Nanostructured Al-doped ZnO-based gas sensor prepared using sol-gel spin-coating method. , 2014, , .		3
78	Structural, optical and electrical characterization of ITO, ITO/Ag and ITO/Ni transparent conductive electrodes. Applied Surface Science, 2014, 288, 599-603.	6.1	33
79	Effect of annealing on structural, optical, and electrical properties of nickel (Ni)/indium tin oxide (ITO) nanostructures prepared by RF magnetron sputtering. Superlattices and Microstructures, 2014, 70, 82-90.	3.1	22
80	InGaN-based multi-quantum well light-emitting diode structure with the insertion of superlattices under-layer. Superlattices and Microstructures, 2013, 60, 201-207.	3.1	4
81	Study of Annealed Nickel (Ni)/Indium Tin Oxide (ITO) Nanostructures Prepared by RF Magnetron Sputtering. Advanced Materials Research, 2013, 832, 695-699.	0.3	3
82	Effects of Pressure Dependence on Nanocolumnar Zinc Oxide Deposited by RF Magnetron Sputtering. Advanced Materials Research, 2013, 832, 787-791.	0.3	3
83	Influence of Substrate Temperature on Morphological and Electrical Properties of Indium Tin Oxide Nanocolumns Prepared by RF Magnetron Sputtering. Advanced Materials Research, 2013, 832, 281-285.	0.3	Ο
84	A Study on the Seebeck Effect of 3,4,9,10-Perylenetetracarboxylic Dianhydride (PTCDA) as a Novel N-Type Material in a Thermoelectric Device. Advanced Materials Research, 2013, 667, 165-171.	0.3	0
85	Influence of RF Magnetron Sputtering Pressure on the Structural, Optical, and Morphological Properties of Indium Tin Oxide Nanocolumns. Advanced Materials Research, 2013, 832, 276-280.	0.3	Ο
86	Effect of Annealing on Surface of Nickel (Ni)/Indium Tin Oxide (ITO) Nanostructures Measured by Atomic Force Microscopy (AFM). Advanced Materials Research, 2013, 832, 51-55.	0.3	0
87	PEDOT:PSS Thin Film as Transparent Electrode in ITO-Free Organic Solar Cell. Advanced Materials Research, 2012, 501, 252-256.	0.3	5
88	Structural properties of InGaN-based light-emitting diode epitaxial growth on Si (111) with AlN/InGaN buffer layer. , 2012, , .		0
89	Electronic properties and electrical characteristics of modified PEDOT:PSS as a buffer layer in organic solar cell. , 2012, , .		0
90	InGaN-based blue LED grown on Si(111) substrate. , 2011, , .		0

#	Article	IF	CITATIONS
91	Effect of AlGaNâ^•GaN Strained-Layer Superlattices Underlayer to InGaN-based Multi-Quantum Wells Grown on Si(111) Substrate by MOCVD. , 2011, , .		1
92	Effect of Al0.06Ga0.94N/GaN Strained-Layer Superlattices Cladding Underlayer to InGaN-Based Multi-Quantum Well Grown on Si(111) Substrate with AlN/GaN Intermediate Layer. Japanese Journal of Applied Physics, 2010, 49, 021002.	1.5	6
93	High performance InGaN LEDs on Si (1 1 1) substrates grown by MOCVD. Journal Physics D: Applied Physics, 2010, 43, 354008.	2.8	25
94	Growth of InGaN-based laser diode structure on silicon (111) substrate. Journal of Physics: Conference Series, 2009, 152, 012007.	0.4	6
95	Electrical and Optical Characterization of Mg Doping in GaN. Advanced Materials Research, 0, 620, 453-457.	0.3	1
96	Compositional and Structural Characterization of Heterostructure InGaN-Based Light-Emitting Diode by High Resolution X-Ray Diffraction. Advanced Materials Research, 0, 620, 22-27.	0.3	4
97	Effects of Oxygen Gas Composition on Nanocolumnar Zinc Oxide Properties Deposited by RF Magnetron Sputtering. Advanced Materials Research, 0, 832, 783-786.	0.3	0
98	Characterization of ITO/Ag and ITO/Ni Bi-Layer Transparent Conductive Electrodes. Advanced Materials Research, 0, 1024, 75-78.	0.3	1
99	Post-Annealing Effects on ITO Thin Films RF Sputtered at Different Thicknesses on Si and Glass. Advanced Materials Research, 0, 925, 411-415.	0.3	3
100	Structural and Optical Properties of Nickel-Doped Zinc Oxide Thin Film on Nickel Seed Layer Deposited by RF Magnetron Sputtering Technique. Advanced Materials Research, 0, 895, 3-7.	0.3	2